where

$$v_1(y_1) = \left(\frac{1}{2}\omega_1{}^2 y_1{}^2 + \lambda y_1\right)\theta\left(-\frac{\Delta I}{2\lambda} - y_1\right) + \left(\frac{1}{2}\omega_1{}^2 y_1{}^2 - \lambda y_1 - \Delta I\right)\theta\left(\frac{\Delta I}{2\lambda} + y_1\right). \tag{18}$$

Probability for the "particle" (infection carrier) transfer can be found in the quasi-classical approximation. We should also assume quasi-stationary transfer. For the case of nonzero temperature we will determine the transfer probability per unit time for an infection carrier as:

$$\Gamma = 2T\frac{\mathrm{Im}\,Z}{\mathrm{Re}\,Z}. \tag{19}$$

Here, Z is a partition function, being the complex value because of the decay. Coherent oscillation [5, 6]), (which we do not consider in the present work) are probable in the case of weak interaction with oscillator environment. To calculate Γ, it is convenient to represent Z in form of the path integral [5, 6]:

$$Z = \prod_{\alpha}\int Dy_1 \int Dy_\alpha \exp\left[-S\{y_1; y_\alpha\}\right]. \tag{20}$$

Since we are not interested in the initial and final oscillator states, it is possible to integrate over the path $y_\alpha(\tau)$, taking the initial conditions $y_\alpha(-\beta/2) = y_\alpha(\beta/2)$, where $\beta \equiv T^{-1}$ and T is "social temperature". Then the action depends only on the path $y_1(\tau)$:

$$S\{y_1\}=\int_{-\beta/2}^{\beta/2} d\tau\left[\frac{1}{2}\dot{y}_1^{\,2}+v(y_1)+\frac{1}{2}\int_{-\beta/2}^{\beta/2} d\tau' K(\tau-\tau')y_1(\tau)y_1(\tau')\right], \tag{21}$$

where

$$v(y_1)=v_1(y_1)-\frac{1}{2}\sum_{\alpha=2}^{N}\frac{C_\alpha^{\,2}}{\omega_\alpha^{\,2}}y_1^{\,2}. \tag{22}$$

Here, the potential is renormalized, or adiabatic potential is introduced. The kernel of an integral term in (21) depends only on the oscillator environment parameters. Under expanding of a kernel $K(\tau)$ in Fourier series, Fourier-coefficients ζ_n are defined as:

$$\zeta_n=\nu_n^{\,2}\sum_{\alpha=2}^{N}\frac{C_\alpha^{\,2}}{\omega_\alpha^{\,2}\left(\omega_\alpha^{\,2}+\nu_n^{\,2}\right)}. \tag{23}$$

where $\nu_n\equiv 2\pi nT$ is the Matsubara's frequency.

Let us perform the following shift of the coordinate y_1

$$q=y_1+\frac{\Delta \mathrm{I}}{2\lambda}. \tag{24}$$

Then

$$v(q)=\frac{1}{2}\omega_0^{\,2}(q+q_0)^2\theta(-q)+\left[\frac{1}{2}\omega_0^{\,2}(q-q_1)^2-\Delta \mathrm{I}\right]\theta(q), \tag{25}$$

where

$$\omega_0^{\,2}=\omega_1^{\,2}-\sum_{\alpha=2}^{N}\frac{C_\alpha^{\,2}}{\omega_\alpha^{\,2}},$$

$$q_0 = \frac{\lambda}{\omega_0^2} - \frac{\Delta I}{2\lambda}, \qquad q_1 = \frac{\lambda}{\omega_0^2} + \frac{\Delta I}{2\lambda}. \tag{26}$$

The form of potential (25) with account of "Euclidean turn" in the instanton approach [5, 6] is represented in Fig. 2.

The partition function Z can be calculated in the quasiclassical approximation. There is a trajectory $q_B(\tau)$ which makes the main contribution to the action $S\{q\}$. This trajectory minimizes the action functional and satisfies the Euler-Lagrange equation:

$$-\ddot{q}_B(\tau) + \frac{\partial v(q_B)}{\partial q_B} + \int_{-\beta/2}^{\beta/2} d\tau' K(\tau - \tau') q_B(\tau') = 0, \tag{27}$$

$q_B(\tau)$ is considered to be a periodic function:

$$q_B(\tau) = q_B(\tau + \beta). \tag{28}$$

The form $q_B(\tau)$ is defined by the "particle" (infectious carrier) motion in the inverted potential, $-v(q)$. A particle begins its motion (in the zero temperature case) on the top of the potential, $(-v(q))$, i.e. in the point $-q_0$, then it passes through the minimum point, $(q_B = 0)$, at $\tau = -\tau_0$ and attains $q_B = q_0$ (in the symmetric potential case) at $\tau = 0$. Then the particle repeats its trajectory in the reverse order. Such a trajectory stands for an instanton. Notice that the instanton action value does not depend on the position of the instanton centre. The time τ_0 is determined by the equation:

$$q_B(\tau_0) = 0 \tag{29}$$

The trajectory $q_B(\tau)$ is represented in Fig. 3. The solution of equation (27) is substantially simplified by the introduction of time τ_0, because the coordinate dependent step-functions may be replaced by the respective time dependent ones:

$$\theta(-q_B)=\theta(-\tau_0-\tau)+\theta(\tau-\tau_0);$$
$$\theta(q_B)=\theta(\tau+\tau_0)-\theta(\tau-\tau_0). \tag{30}$$

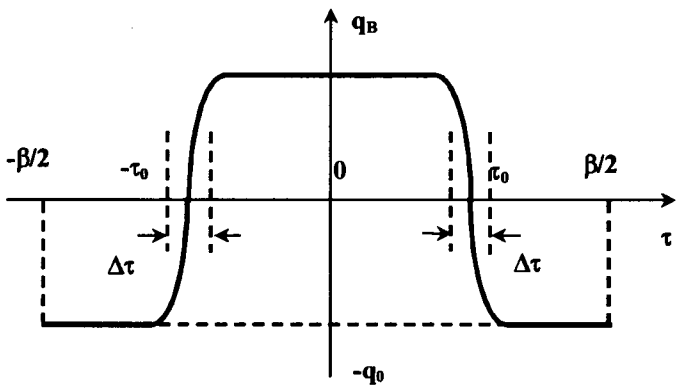

Fig. 3. The instanton trajectory $q_B(\tau)$. τ_0 is the instanton centre, $\Delta\tau$ is the instanton width.

Let us expand $q_B(\tau)$ in Fourier series:

$$q_B(\tau)=\beta^{-1}\sum_{n=-\infty}^{\infty}q_n\exp(i\nu_n\tau). \tag{31}$$

Expanding θ-functions and kernel $K(\tau)$ in Fourier series we obtain the equation determining the Fourier-coefficients q_n . This equation may be solved exactly, and we find:

$$q_B(\tau) = -q_0 + \frac{2(q_0+q_1)\tau_0}{\beta} + \frac{2\omega_0^2(q_1+q_0)}{\beta}\sum_{n=1}^{\infty}\frac{\sin\nu_n\tau_0\cdot\cos\nu_n\tau}{\nu_n\left(\nu_n^2+\omega_0^2+\zeta_n\right)}, \quad (32)$$

where $\nu_n = 2\pi n/\beta$ is Matsubara frequency, and ζ_n is defined by equation (23). Substituting (32) into the expression for action, we obtain:

$$S_B = 2\omega_0^2(q_0+q_1)q_0\tau_0 - \frac{2\omega_0^2(q_0+q_1)^2\tau_0^2}{\beta} -$$

$$-\frac{4\omega_0^4(q_0+q_1)^2}{\beta}\sum_{n=1}^{\infty}\frac{\sin^2\nu_n\tau_0}{\nu_n^2\left(\nu_n^2+\omega_0^2+\zeta_n\right)}. \quad (33)$$

Thus, quasiclassical action in the one-instanton approximation is analytically found. In the simplest case without interaction with environment, i.e. ζ_n=0, τ_0 is determined from equations (29) and (32):

$$\tau_0 = \frac{1}{2\omega_0}Arcsh\left[\frac{q_0-q_1}{q_0+q_1}\,sh\frac{\omega_0\beta}{2}\right] + \frac{\beta}{4}. \quad (34)$$

The action may be found from expressions (33) and (34):

$$S_B = \frac{\omega_0\left(q_1^2-q_0^2\right)}{2}Arcsh\left[\frac{q_1-q_0}{q_1+q_0}\,sh\frac{\omega_0\beta}{2}\right] - \frac{\omega_0^2\left(q_1^2-q_0^2\right)}{4}\beta +$$

$$+\frac{\omega_0(q_1+q_0)^2}{2}\left\{\frac{ch\frac{\omega_0\beta}{2} - \left[1+\left(\frac{q_1-q_0}{q_1+q_0}\right)^2 sh^2\frac{\omega_0\beta}{2}\right]^{1/2}}{sh\frac{\omega_0\beta}{2}}\right\}. \quad (35)$$

In the symmetric case

$$S_B = 2\omega_0 q_0^{\,2}\, th\frac{\omega_0\beta}{4}. \qquad (36)$$

Thus, we have completed construction of our model, and the transfer probability Γ (for infectious carrier transfer) with the exponential accuracy can be estimated as $\Gamma \square \exp(-S)$. Below, we turn to analysis of the results.

3. Results and discussion

Dependence of the transfer probability Γ (for infectious carrier) on "social temperature" T^* is depicted on Fig. 4. This probability is very sensitive to the local oscillator mode frequency and to the interaction constant with the heat bath (or contact environment), Fig. 5. These results are quite expectative: effectiveness of interaction increases with the oscillator frequency rise that gives corresponding growth in the transfer energy (for infectious carrier) and takes the transfer probability increase ("transition" from curve 1 to curve 2, Fig. 5); increase of the interaction constant leads to increase in "viscosity" (or dissipation measure) of the contact environment, and this reduces the transfer probability for infectious carrier ("transition" from curve «1» to curve «3», Fig. 5). Also, in Fig. 5 one can observe the "blockage" effect. The "blockage" effect for the infectious diseases transfer has been demonstrated in the case when peak values (in the population density) are equal to each other (asymmetry parameter equals to 1); and under condition when "social temperature" is low. Existence of such

effect essentially depends on the environment "activity" (social and prophylactic).

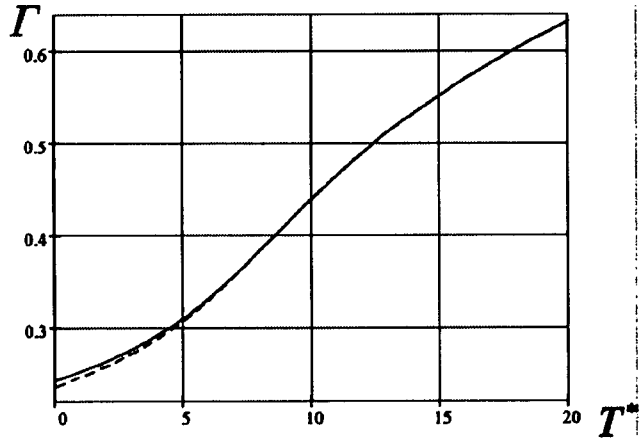

Fig. 4. Dependence of the transfer probability Γ (for infectious carrier) on "social temperature" T^*.

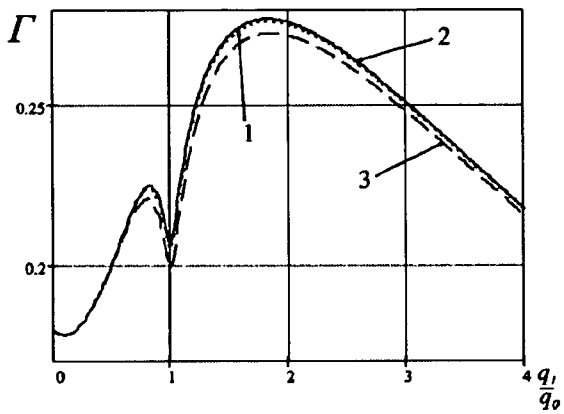

Fig. 5. Dependence of the transfer probability Γ (for infectious carrier) on the asymmetry parameter $\frac{q_1}{q_0}$ (for population density profile).

In summary, in this paper applicability of the instanton approach to modeling of the infectious diseases transfer dynamics has been shown on an example

of tuberculosis. Controllable features of influence on the infectious diseases spread rate have been revealed. In case of "blockage" effect, influence of the slow-changeable factors (such as the population density profile) has been accounted for; also we have shown the role of such dynamical factors as "social temperature" and other parameters of the infectious transfer environment in the infectious transfer control.

Acknowledgements. This work has been partly supported by grants: JSPS grant ID N S-05052; grant "Iryokikicenter", "Nano Medicine Supporting Program". The authors are grateful to Prof. K. Suzuki for the support of this work.

References

[1] Debanne S.M., Bielefeld R.A., Cauthen G.M., Daniel T.M., Rowland D.Y.,. "Multivariate Markovian Modeling of Tuberculosis: Forecast for the United States', Emerging Infectious Diseases, **6**, 148 – 157 (2000).

[2] Krevchik V.D., Novikova T.V., Semenov M.B., Yamamoto K., "Nonlinear 1D and 2D-dynamics for the infectious diseases transfer with possible applications for tubercular infection", Proc. of the Second International Symposium on Transmission Models for Infectious Diseases, 19-20 January, 2006, National Institute of Infectious Diseases, Tokyo, Japan, p. 14.

[3] Koopman J.S., "Infection Transmission Science and Models," Japanese Journal of Infectious Diseases, **58**(6), S3 - S8 (2005).

[4] Suzuki K., Yamamoto K., Yoshikura H., International Symposium of Infectious Agent Transmission Model Building – Focusing on Assessment of

Risk to Communities. Japanese Journal of Infectious Diseases, **58**(6), S1 - S2 (2005).

[5] A.A. Ovchinnikov, Yu.I. Dakhnovskii, V.Ch. Zhukovsky, V.D. Krevchik, M.B. Semenov, A.I. Ternov, and A.K. Aringazin, *Introduction to Modern Mesoscopic Phenomena*, Penza, Penza State Univ., 2003, 610 pages. (in Russian)

[6] A.A. Ovchinnikov, Yu.I. Dakhnovskii, V.D. Krevchik, M.B. Semenov, and A.K. Aringazin, *Principles of Driven Modulation of Low-Dimensional Structures*, Moscow, UNC DO, 2003, 510 pages. (in Russian)

Microbiol. Immunol., 51(5), 551–566, 2007

Editor-Communicated Paper

Trafficking of QD-Conjugated MPO-ANCA in Murine Systemic Vasculitis and Glomerulonephritis Model Mice

Akiyoshi Hoshino[1,2,3], Tomokazu Nagao[1], Toshiko Ito-Ihara[1,4,5,6], Akiko Ishida-Okawara[1], Kazuko Uno[5], Eri Muso[6], Noriko Nagi-Miura[7], Naohito Ohno[7], Kazuhiro Tokunaka[8], Shiro Naoe[9], Hiroshi Hashimoto[10], Masato Yasuhara[3], Kenji Yamamoto[2,3], and Kazuo Suzuki*[,1]

[1]Department of Bioactive Molecules, National Institute of Infectious Diseases, Shinjuku-ku, Tokyo, 162–8640 Japan, [2]International Clinical Research Center, Research Institute, International Medical Center of Japan, Tokyo, Japan, [3]Department of Pharmacokinetics and Pharmacodynamics, Hospital Pharmacy, Tokyo Medical and Dental University Graduate School, Bunkyo-ku, Tokyo, 113–8520 Japan, [4]Department of Nephrology and Cardiovascular Medicine, Graduate School of Medicine, Kyoto University, Kyoto, 606–8507 Japan, [5]Louis Pasteur Center for Medical Research, Kyoto, 606–8225 Japan, [6]Kitano Hospital Medical Research Institute, Osaka, 530–8480 Japan, [7]Laboratory for Immunopharmacology of Microbial Products, School of Pharmacy, Tokyo University of Pharmacy and Life Science, Hachioji, Tokyo, 192–0392 Japan, [8]Nippon Kayaku Co., Chiyoda-ku, Tokyo, 102–8172 Japan, [9]Department of Pathology, Toho University Ohashi Hospital, Meguro-ku, Tokyo, 153–8515 Japan, and [10]Department of Rheumatology and Internal Medicine, Juntendo University School of Medicine, Bunkyo-ku, Tokyo, 113–8421 Japan

Communicated by Dr. Hidechika Okada: Received February 8, 2007. Accepted February 27, 2007

Abstract: **In systemic vasculitis, the serum level of myeloperoxidase (MPO)-specific anti-neutrophil cytoplasmic autoantibodies (MPO-ANCA) is significantly elevated with the progression of disease. We have established a model of murine systemic vasculitis by administration of MPO-ANCA and fungal mannoprotein to C57BL/6 mice. We examined the role of MPO and MPO-ANCA in the pathogenesis of glomerulonephritis and systemic vasculitis in this model using quantum dots (QDs). We demonstrated that QD-conjugated MPO-ANCA (ANCA-QD) visualized the translocation of MPO on the neutrophil membrane surface after stimulation with proinflammatory cytokines. We also observed that MPO translocation on neutrophils in both patients with rapid progressive glomerulonephritis and these model mice without any stimulation, suggesting that MPO translocation is certain to contribute to the development of glomerular lesion. In addition, blood flow on the kidney surface vessel was significantly decelerated in both SCG/Kj mice and this model, suggesting that ANCA induces the damage of blood vessel. These results indicate that MPO-ANCA and surface-translocated MPO on the activated neutrophils coordinately plays essential roles in the initial steps of the glomerulonephritis.**

Key words: **Neutrophils, Autoimmunity, Fungal, Autoantibodies, Cytokines**

Neutrophils act as the initial innate immune response against invading microorganisms to produce reactive oxygen species by releasing their lysosomal enzymes, including peroxidases (47, 48). One of them, myeloperoxidase (MPO), is an essential molecule in the initiation and execution of the acute inflammatory response and subsequent resolution of fungal, bacterial, and viral infection (1, 2, 8, 26, 32). However, excessive release of MPO is responsible for severe injury to

*Address correspondence to Dr. Kazuo Suzuki, Department of Bioactive Molecules, National Institute of Infectious Diseases, Toyama 1–23–1, Shinjuku-ku, Tokyo 162–8640, Japan. Fax: +81–3–5285–1111. E-mail: ksuzuki@nih.go.jp

Abbreviations: ANCA, anti-neutrophil cytoplasmic autoantibody; CAWS, *C. albicans* water-soluble mannoprotein and β-glucan complex; H&E, hematoxylin/eosin; MPO, myeloperoxidase(s); MPO-ANCA, MPO-specific anti-neutrophil cytoplasmic autoantibody; PR-3, proteinase-3; QD, quantum dot; rmMPO, recombinant murine MPO; RPGN, rapidly progressive glomerulonephritis; SCG, spontaneous crescentic glomerulonephritis; SCG/Kj, SCG-forming mouse/Kinjoh.

organs and blood vessels; the neutrophils infiltrated into the inflammatory vascular lesion are believed to contribute to the progression of vasculitis (23). In particular, the MPO-specific anti-neutrophil cytoplasmic autoantibody (MPO-ANCA) is significantly involved in the development of various kinds of vasculitis, ANCA-associated rapid progressive glomerulonephritis (RPGN), and microscopic polyangiitis (11, 15, 30, 34). We and other groups have demonstrated that MPO is a major antigen for MPO-ANCA production by using MPO-deficient mice (3, 19), and adoptive transfer of MPO-reactive splenocytes into Rag2-deficient mice resulted in crescentic glomerulonephritis with high MPO-ANCA titer (53). Furthermore, we have shown the contribution of activated neutrophils in renal lesions using spontaneous crescentic glomerulonephritis-forming mouse/Kinjoh (SCG/Kj) glomerulonephritis model mice (12, 20). In the early phase of glomerulonephritis, the spontaneous release of MPO from neutrophils was increased, indicating that activated neutrophils contribute to the development of active crescentic lesion in SCG/Kj mice. On the other hand, it was reported that a murine vasculitis model, which is induced by the administration of *Candida albicans*-derived glycoprotein, was accompanied by a high titer of MPO-ANCA in serum as well as that of SCG/Kj (20). We also reported that administration of *Candida albicans* water-soluble mannoprotein (CAWS) induces coronary arteritis similar to Kawasaki Disease (36, 38). *C. albicans* infection shows a lethality resembling anaphylactic fungal sepsis due to the release of some types of polysaccharide fraction into the blood (28) and the subsequent production of proinflammatory cytokines (21). Thus, it is assumed that activated neutrophils may contribute to the development of ANCA-related systemic vasculitis due to the association of MPO-ANCA with MPO antigen (49).

Proteinase-3 (PR3), which is another autoantigen in neutrophils, is known to be translocated on the surface of activated neutrophils. In contrast, the surface translocation of MPO in living neutrophils has not been investigated morphologically by fluorescent microscopy, whereas detection by flow cytometric detection has been reported (14); detection of surface-translocated MPO on living neutrophils was difficult due to its oxidative enzymic activity (6). Therefore, a fluorescent probe with far-bright emission has been required for a long time to observe the MPO on living neutrophils. Recently, fluorescent nanocrystal quantum dots (QDs) have been applied to molecular biology because of their greater and far longer fluorescence; they are now widely used in biotechnological and medical applications (7, 10, 51, 52).

In the present study, we conjugated QDs with MPO-ANCA, and revealed the trafficking of MPO-ANCA *in vivo*. Thus, we here established the mouse models of systemic vascular inflammation to clarify the initial activation step of chronic autoimmune inflammation and systemic vasculitis.

Materials and Methods

Mice. C57BL/6J mice were purchased from Japan Clea, Inc. (Tokyo). SCG/Kj were provided by Nippon Kayaku Co. (Tokyo) and maintained in our animal facility at the National Institute of Infections Diseases. Male mice over 12 weeks old were used as aged mice. All experiments were performed according to the Guidelines for Laboratory Animal Experiments in Research and with the approval of the local ethics committee at the National Institute of Infectious Diseases.

Reagents. FMLP (formyl-Met-Leu-Phe oligopeptides) was purchased from the Peptide Institute (Osaka, Japan). Recombinant human TNF-α and IL-1β were purchased from Chemicon (Temecula, Calif., U.S.A.). Mouse complement was purchased from Rockland Immunochemicals, Inc. (Gilbertsville, Pa., U.S.A.). The MPO-ANCA used in study was polyclonal anti-rmMPO antibody (anti-rmMPO Ab) prepared by immunization with recombinant murine MPO, which is produced by *Escherichia coli* transfected with cDNA of murine MPO, as described previously (22, 36), and the produced MPO-ANCA have an ability to cross-react to both murine and human MPO molecules. QDs (ZnS-coated CdSe nanocrystal; approximately 642 nm red fluorescence) were synthesized chemically (17) and conjugated with MPO-ANCA via their sulfhydryl group using SMCC (Pierce Biotechnology, Rockfold, Ill., U.S.A.) (16). The QD-conjugated Ab produced bound physically to QDs (ANCA-QD) and was detected by transmission electron microscopy with osmium tetroxide (OsO_4)-negative staining. The antibody captured on QD measured with the Bradford reagent (Bio-Rad Laboratories, Hercules, Calif., U.S.A.) with the standard curve of bovine serum albumin indicated that each ANCA-QD had approximately 8.5 Abs per QD nanocrystal (data not shown, see ref. 18). The function of ANCA-QD was checked by fluorescent Western blotting and histochemical analysis (39). CAWS (*Candida albicans*-derived water-soluble mannoprotein and β-glucan complex) was extracted from the culture supernatant of *C. albicans* (IFO 1385) which was prepared as previously described (29).

Neutrophil extraction, surface MPO stain and flow cytometric analysis. Murine neutrophils were collected from the peritoneal cavity of C57BL/6 and the aged (13 wks, male) SCG/Kj mice 3 hr after i.p. injection with

8% casein/PBS. Human neutrophils were collected from a patient with MPO-ANCA-associated RPGN and a healthy control, as described previously (9). In brief, human neutrophils were isolated from heparinized peripheral blood with Lymphoprep™ (Axis-Shield, Dundee, U.K.), 1.5% dextran (200 kDa), and retained erythrocytes were removed with lysis buffer [0.75% NH_4Cl in 20 mM Tris-HCl (pH 7.6)]. Collected neutrophils were preincubated at 37 C with Hanks' balanced salt solution (HBSS) for 10 min, and plated on a prewarmed 12-μm-thick coverslip (Matsunami Glass Industries, Osaka, Japan) attached with a silicone-made rubber well plate for 10 min. After stimulation with proinflammatory cytokines, neutrophils were immediately fixed with 1% paraformaldehyde/PBS and permeabilized by 0.1% Triton-X 100 if needed. Neutrophils were then blocked for 30 min with 1% bovine serum albumin (Sigma Cat#A6003; without serum MPO molecules) and then stained with ANCA-QD. Images were acquired with a CCD camera DP-70 (Olympus, Japan) under fluorescent microscopy IX-81 (Olympus) equipped with a LP (>610 nm) filter unit. For flow cytometry, collected neutrophils were stimulated for 10 min, stained with ANCA-QD and anti-human CD11b mAb (clone D12, PharMingen BD, San Diego, Calif., U.S.A.). Unfixed neutrophils were immediately analyzed by FACS Calibur (BD Biosciences).

ANCA-induced systemic vasculitis model and movie caption (intravital fluorescence videomicroscopy). C57BL/6J (male, 9 wks old) mice were injected i.v. with 1 mg of MPO-ANCA after pretreatment with i.p. injection of CAWS (4 mg/mouse) on day 0. On day 5, MPO-ANCA (1 mg/mouse) were injected again as secondary stimuli (see Fig. 1a). For imaging, 250 μg of ANCA-QD was added to the naïve MPO-ANCA in the case of second infection. Polyclonal mouse IgG was used as a negative control. After secondary stimulation, mice were sacrificed moribund on day 10. Bladder urine was collected to measure leaked protein and MPO-ANCA.

For intravital fluorescence videomicroscopy, mice were anesthetized with s.c. injection of ketaral solution (85 mg/kg) supplemented with xylazine (17 mg/kg). Mice were set on the videomicroscopy stage at 37 C with a heating pad, and renal surface microcirculation on the exposed right kidney was observed through a flank incision with RITC-dextran probes (5 mg/kg, i.v.; Sigma). The movie was captured by a video camera with image intensifier (Hamamatsu Photonics Corp., Hamamatsu, Japan) and recorded by a DVD video recorder (Hitachi, Ltd., Tokyo). The status of the superficial blood flow was determined in each microvessel by the following criteria: (1) Normal, capillaries with fast blood flow in which each erythrocyte could not be recognized; (2) occlusion, capillaries completely occluded by erythrocytes; and (3) abnormal, capillaries that show slow blood flow or repeat flow and stop.

Histology. For immunohistochemical stain, hematoxylin/eosin (H&E), and Periodic Acid Schiff (PAS) histology, collected kidney, liver, lung, and spleen were immediately washed, fixed with 10% formaldehyde neutralized solution for 4 hr. After the organs were incubated with 20% sucrose overnight, the cryosection was sliced to 4-μm thickness and affixed to a glass slide (Matsunami Glass Industries). Neutrophils were stained with FITC-conjugated anti-Gr1 mAb (PharMingen BD) or FITC or phycoerythrin (PE)-conjugated anti-CD11b mAb M1/70 (PharMingen). The disease score of the kidney lesion was evaluated by area glomerulus area, number of neutrophil infiltrating into the glomerulus, and cell proliferation in the glomerulus, based on Fischer's protected least significance difference (PLSD) test.

Multiple cytokine assay. Twelve microliters of undiluted mouse serum samples were used for parallel detection of 18 cytokines and chemokines in murine serum using the Bio-Plex® Cytokine Assay 20-Plex kit (Bio-Rad Laboratories) according to the manufacturer's protocol, and analyzed by the Bio-Plex Luminex 100 XYP instrument for analysis. Cytokine concentrations were calculated using Bio-Plex Manager 3.0 software with a five-parameter curve-fitting algorithm applied for standard curve calculations.

Statistical analysis. Data presented as mean ± 1 SD were compared using the two-tailed student's *t*-test and Fischer's PLSD test (Fig. 3) with KaleidaGraph 4.0 (Synergy Software, Reading, Pa., U.S.A.). *P* values <0.05 were regarded as significant.

Results

Establishment of a Murine Systemic Vasculitis Model Associated with MPO-ANCA

We have previously demonstrated that MPO-ANCA is enhanced in SCG/Kj mice showing spontaneous glomerulonephritis (37). Hence, MPO-ANCA has a key role in the development of systemic inflammation. To clarify the role of MPO-ANCA at the initial phase of autoimmune diseases, we need to create a novel systemic vasculitis model associated with MPO-ANCA. We have established a murine coronary arteritis model using CAWS fungal mannoprotein to C57BL/6 (36, 38), and this model also increased ANCA titer at a slow rate. To mimic higher ANCA-titer of systemic inflammation, we injected MPO-ANCA to the CAWS-pre-

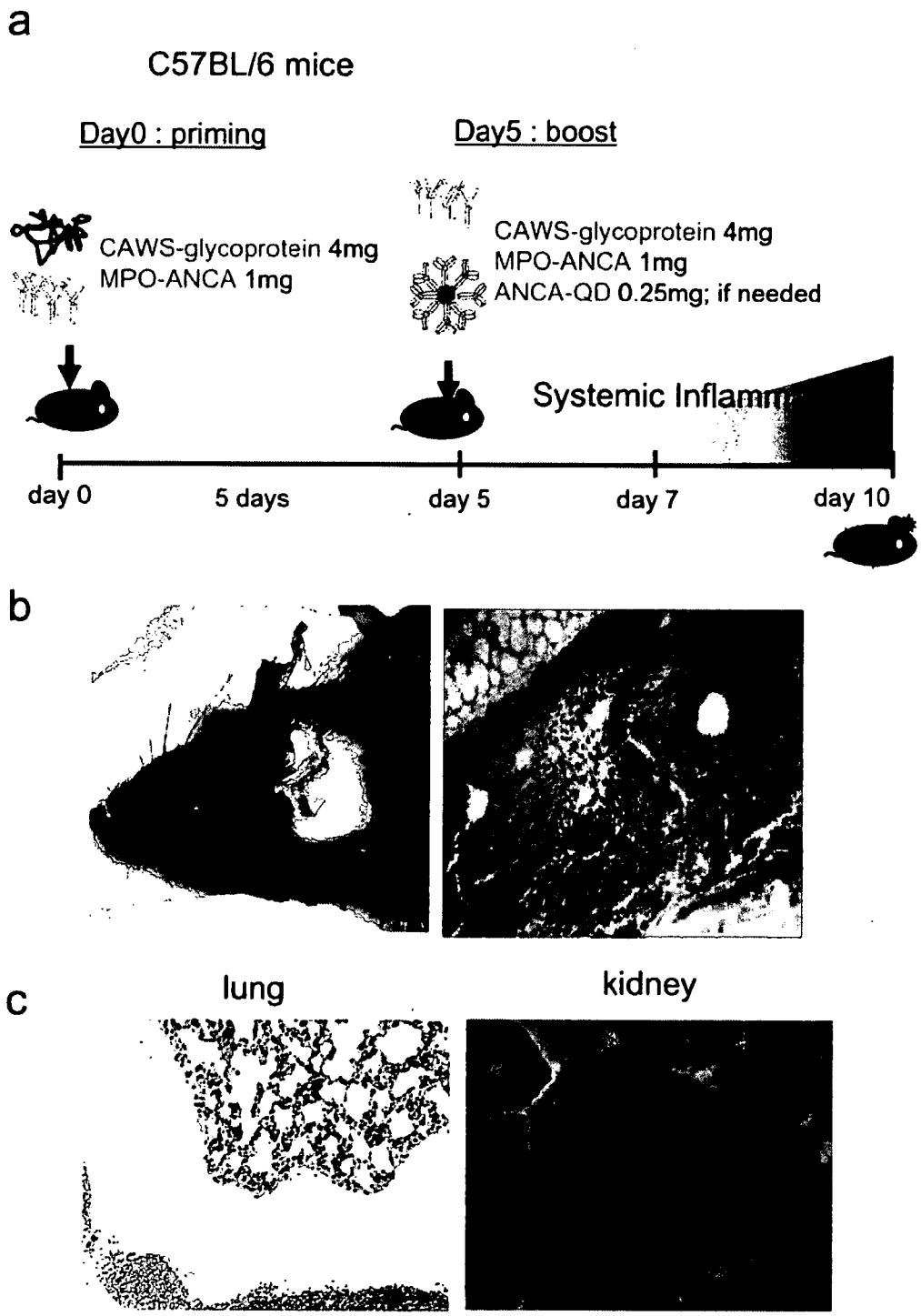

Fig. 1. Experimental procedure of MPO-ANCA-induced murine systemic vasculitis model. *a*, Schematic illustration of MPO-ANCA and CAWS-induced murine experimental systemic vasculitis model. C57BL/6J mice (male, 9 wks old) were injected i.v. with MPO-ANCA (1 mg of Ab/mouse) after pretreatment with 4 mg of i.p. injection of CAWS mannoprotein. On day 5, MPO-ANCA (1 mg naïve Ab/mouse, addition with an additional 250 μg/ml ANCA-QD if needed) was injected i.v. again to develop systemic vasculitis. *b*, Massive systemic inflammation in ear occurred in a mouse treated with CAWS and FMLP in addition to MPO-ANCA. The snapshots were taken 16 hr after secondary stimulation. Histochemical feature of inflamed auricle of systemic vasculitis mice was observed by PAS stain. Original magnification, ×200. *c*, H&E staining of the lung and kidney lesion of systemic vasculitis mice. Original magnification, ×200.

a

		0hr	3hr	18hr	24hr
Urinary protein [mg/dl]	Control IgG	<30	30	30	<30
	MPO-ANCA	<30	300	30-100	100
Occult blood	Control IgG	—	—	—	—
	MPO-ANCA	—	+	—	—

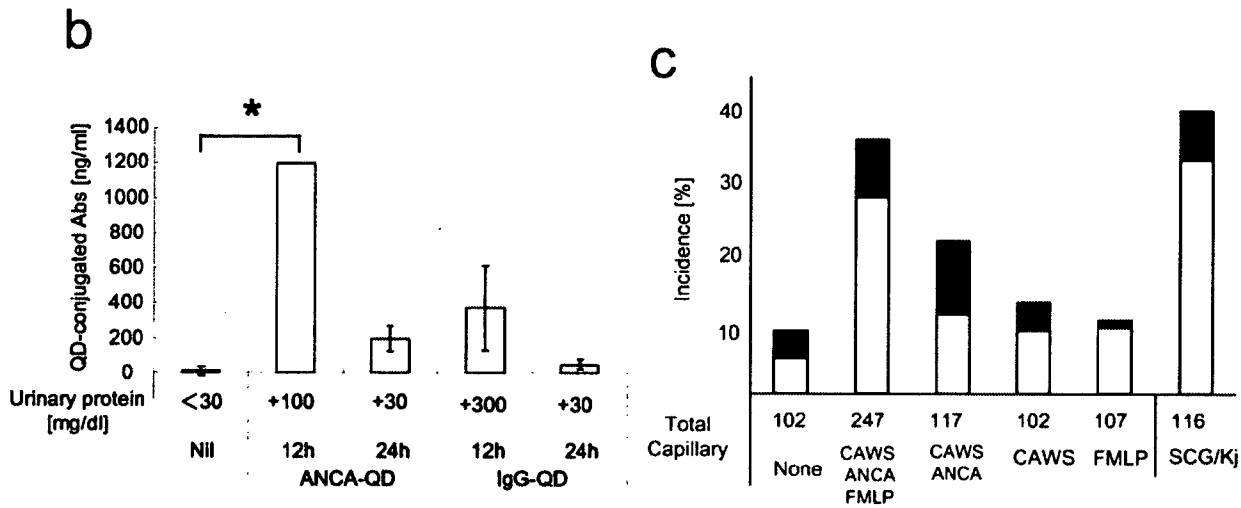

Fig. 2. Clinical feature of MPO-ANCA-induced systemic vasculitis mice. *a*, Urinary protein and occult blood leaked out from injured glomeruli were measured after second stimulation. *b*, Leaked ANCA-QD into urine was measured by fluorescent spectrometer. Ab concentration in collected urine was calculated based on the fluorescent standard curve of ANCA-QD. The data are presented as the mean ± standard deviation of duplicate samples (n=3). Total urinary protein was measured at the same time. *c*, The incidence of capillary with diminished blood flow (open column) and with the occlusion of renal circulation (filled column) was calculated. The counted capillary numbers in each kidney are displayed under each column.

treated mice in order to induce severe inflammation (Fig. 1a). As a result, massive systemic inflammation was observed, especially in severe necrotic auricularitis (Fig. 1b). In this model, approximately one-third mice died due to the hemorrhage inside the thorax (Fig. 1c). Moreover, histological analysis indicated that the inflammation was due to enhanced activation of infiltrating neutrophils in both lung and kidney (Fig. 1c). Next, we assessed the renal function of the glomerulonephritis. A renal dysfunction with massive proteinuria was detected from 2 hr after administration of MPO-ANCA (Fig. 2a). In addition, when ANCA-QD was additionally injected with MPO-ANCA in order to investigate the leaked autoantibody, QD-specific fluorescence was detected in the urine, whereas treatment with control IgG with CAWS promotes less proteinuria (Fig. 2b). To support this, in particular, the incidence ratio of capillary with diminished blood flow (open column) and with occlusion of kidney circulation (filled column) was increased after combined stimulation of MPO-ANCA and CAWS mannoprotein (Fig. 2c). The systemic inflammation was enhanced by costimulation of FMLP, implying that activated neutrophils significantly concerned with the glomerular lesion.

To further assess the systemic inflammation, histological staining of kidney and lung were performed. The neutrophils were infiltrated into glomeruli after MPO-ANCA injection (Fig. 3a, lower panel). With the infiltration of neutrophils, mesangiolysis with neutrophil infiltration was occurred in glomeruli on day 6, followed by significant spreading of the area of glomeruli (Fig. 3a and 3b). However, there is no intrinsic cell-proliferation in glomeruli (Fig. 3c), implying that MPO-ANCA injection with CAWS are associated with not mesangioproliferation but extensive widening of the subendothelial space, and mesangiolysis is thought to follow the endothelial injury (33).

Concurrently, massive pulmonary hemorrhage with

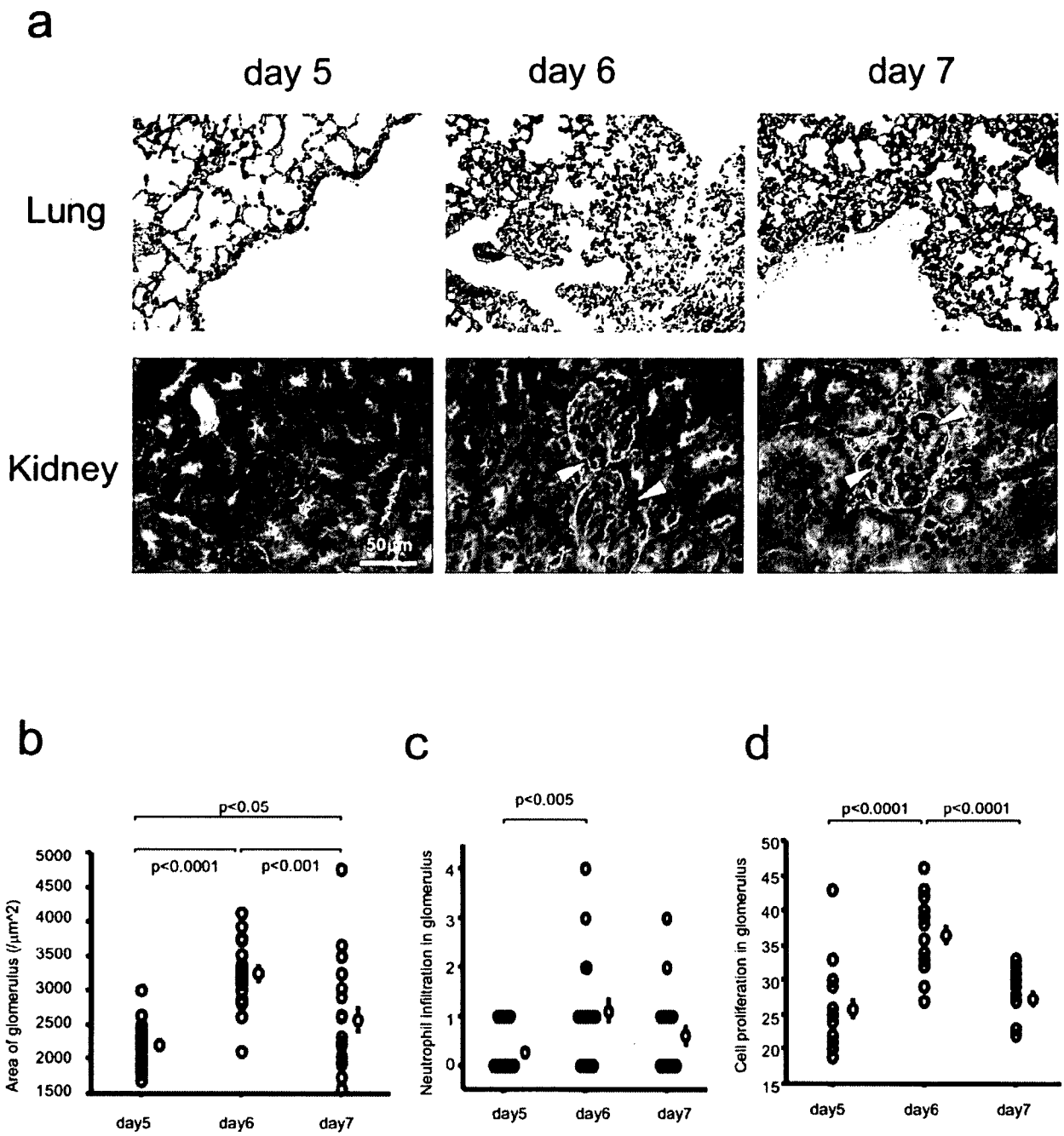

Fig. 3. Severe glomerular mesangiolysis with neutrophil infiltration was observed in experimental systemic vasculitis. PAS staining of kidney and lung in mice receiving MPO-ANCA (1 mg of naïve Ab with an additional 250 μg/ml of ANCA-QD for imaging). After the second injection with ANCA-QD, kidney and lung were collected on days 6 and 7, then embedded in paraffin sections to 4-μm thickness. (*a*) PAS staining of lung (upper) and kidney (lower). The arrowhead shows the infiltrated neutrophils. Magnification, ×400. (*b–d*) Histological score of glomerular lesions, neutrophil infiltration, and intrinsic cell proliferation in glomerulus in kidney were assessed. The data in red show an average ± standard deviation of kidney lesion (n=20). Significance in figures was calculated based on Fischer's PLSD test.

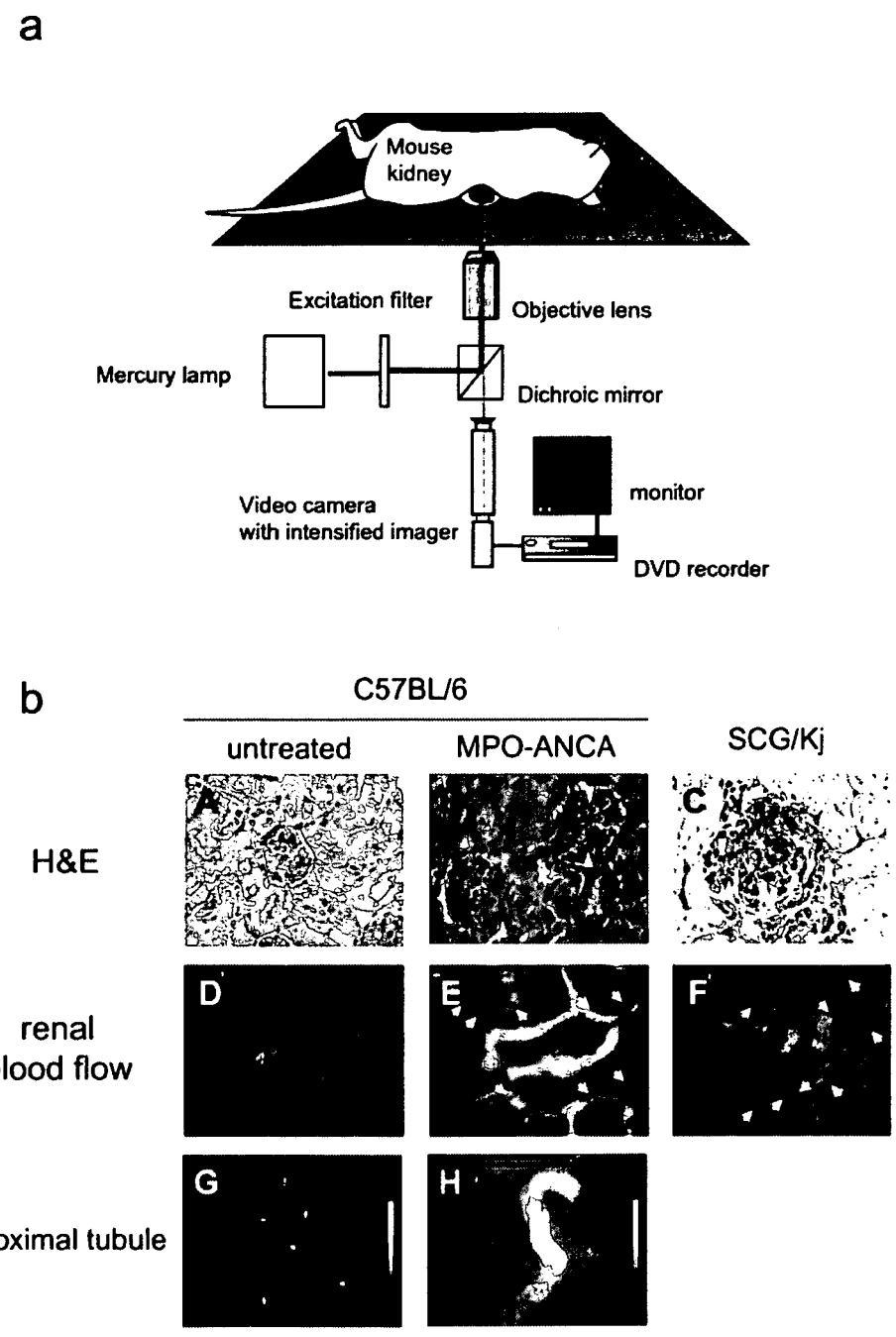

Fig. 4. MPO-ANCA administration with CAWS mannoprotein induces massive systemic vasculitis with severe renal blood deceleration. *a*, Schematic illustration of intravital videomicroscopy in MPO-ANCA-induced murine systemic vasculitis model. C57BL/6J mice were injected i.v. with MPO-ANCA twice (on day 0 and day 5) after pretreatment with 4 mg of i.p. CAWS injection. On day 10, intravital fluorescence videomicroscopy of renal surface microcirculation was performed on a fluorescent microscopy stage with a heating pad. Renal blood flow of systemic vasculitis mice described above was visualized by i.v. co-injection of RITC-dextran probes (5 mg/kg, i.v.; Sigma-Aldrich). *b*, H&E staining (top, *A–C*), renal blood flow (middle, *D–F*) of MPO-ANCA received and aged SCG/Kj mice developing glomerulonephritis. Arrowheads in H&E images indicate the infiltrated neutrophils. Original magnification, ×200. A representative histology from 10 examinations is presented and similar histological findings were obtained in other examinations. *Right*, time-lapse shots of renal blood flow by intravital fluorescent videomicroscopy. The arrows indicate leukocyte adhesion on the renal vessel. Serum proteins and MPO-ANCA were leaked out from collapsed glomeruli to the proximal tubule (bottom *G*, *H*). The RITC-dextran probe leaked to the proximal tubule in control mice and MPO-ANCA-received mice was detected.

severe neutrophil infiltration was observed in concert with the development of systemic inflammation (Fig. 3a, upper panel). In contrast, no inflammation was induced when control murine IgG were administered on day 5 (as a negative control IgG to CAWS-pretreated mice on day 0). In addition, treatment with only MPO-ANCA also showed neither lung inflammation nor mesangioproliferated glomeruli (data not shown). These result suggested that the combinational injection of MPO-ANCA with CAWS can induce the severe systemic inflammation with neutrophil infiltration.

Deceleration of Renal Blood Flow Due to Neutrophil Infiltration into Collapsed Glomeruli

To investigate whether vascular lesion with renal dysfunction occurred in kidney, we visualized the blood flow on the renal surface vessel using intravital fluorescent videomicroscopy (Fig. 4a). Simultaneous costimulation of MPO-ANCA dramatically decelerated blood flow in the kidney surface vessel with leukocyte adhesion, whereas mice administered only CAWS or MPO-ANCA alone still remained (Fig. 4b, inset E). Decelerated circulation was also observed in SCG/Kj mice without any stimulation (Fig. 4b, inset F). The dysfunction of kidney circulation also affected urogenous activity; a RITC-dextran probe injected into the circulating blood stream visualized the leakage of serum protein from the proximal tubule to the urine (Fig. 4b, inset G and H). This is consistent with results showing that a large amount of ANCA-QD was detected in urine (Fig. 2B). These results suggest that MPO-ANCA have a potential to cause glomerular lesion via neutrophil activation in concert with fungal mannoprotein.

Neutrophils of ANCA-Associated Glomerulonephritis Model Mice Shows Increased MPO Translocation to the Neutrophil Membrane

SCG/Kj mice are well known to spontaneously develop crescentic glomerulonephritis and systemic vasculitis (20, 25, 37), and we previously investigated in SCG/Kj mice the correlation of elevated ANCA titer after 10 weeks with the development of spontaneous vasculitis (36). Therefore, activated neutrophils were believed to translocate MPO on their surface as same as PR3. We stained neutrophils obtained from SCG/Kj mice, control C57BL/6, and ANCA-injected C57BL/6 mice with ANCA-QD. When neutrophils were stained with ANCA-QD, MPO was detected as translocated form on the surface membrane in almost 30% of neutrophils when they were primed with FMLP, whereas neutrophils of C57BL/6 mice without stimulation showed no MPO translocation (Fig. 5a). Thus, healthy murine neutrophils (C57BL/6) have an ability to translocate their concealed MPO to the plasma membrane only after priming with FMLP *in situ*. It is noteworthy that even nonstimulated neutrophils from both SCG/Kj and ANCA-treated C57BL/6 mice have translocated the MPO on their surface membrane. To support this, neutrophils of healthy volunteers and patients with ANCA-associated RPGN showed profiles similar to those of mice (data not shown). These observations indicate that the irregular MPO translocation on the neutrophils is involved in the MPO-ANCA-associated glomerulonephritis in mice as well as in humans. This result prompted us to investigate whether MPO translocated on the neutrophil surface by stimulation with CAWS and various proinflammatory cytokines, because ANCA-mediated neutrophil activation resulted in the generation of reactive oxygen species and degradation following cytokine production (42). Surface MPO translocation in normal human neutrophils was observed by FMLP and proinflammatory cytokines such as TNF-α, IL-1β and IL-8 (Fig. 5b). In addition, MPO translocation on neutrophils was observed at a concentration of 10^{-8} M FMLP, that is consistent with the result that human neutrophils show chemoattraction on FMLP at 10^{-8} M (18). However, CAWS stimulation induces no MPO translocation (Fig. 5b), implying that CAWS mannoprotein has no ability to activate neutrophils directly. These results indicate that the constitutive activation of neutrophils may be induced by proinflammatory cytokines on patients with ANCA-associated RPGN.

QD-Conjugated MPO-ANCA Are Detected on Activated Neutrophils in ANCA-Induced Systemic Vasculitis Mice

We visualized the trafficking of MPO-ANCA by the fluorescence of ANCA-QD. To investigate whether MPO-ANCA can be observed in inflammatory lesion, 1 mg of ANCA-QD were injected to the aged (13 wks old) SCG/Kj mice with developed glomerulonephritis. QD luminescence was widely distributed by blood flow and observed in organs including spleen, lung, liver, and kidney (Fig. 6a). Notably in kidney, ANCA-QD was specifically accumulated in the collapsed glomeruli 24 hr after administration of ANCA-QD into SCG/Kj mice (Fig. 6b). In contrast, when control IgG-QD were administered as a negative control antibody, no QD luminescence was observed in glomeruli despite the glomerulonephritis had already developed (Fig. 6c).

Next we visualized the trafficking of MPO-ANCA in our established murine systemic vasculitis model. To investigate whether MPO-ANCA is associated and reacted with activated neutrophils at glomerular lesion with neutrophil infiltration, 25% ANCA-QD were co-injected with MPO-ANCA when mice was stimulated

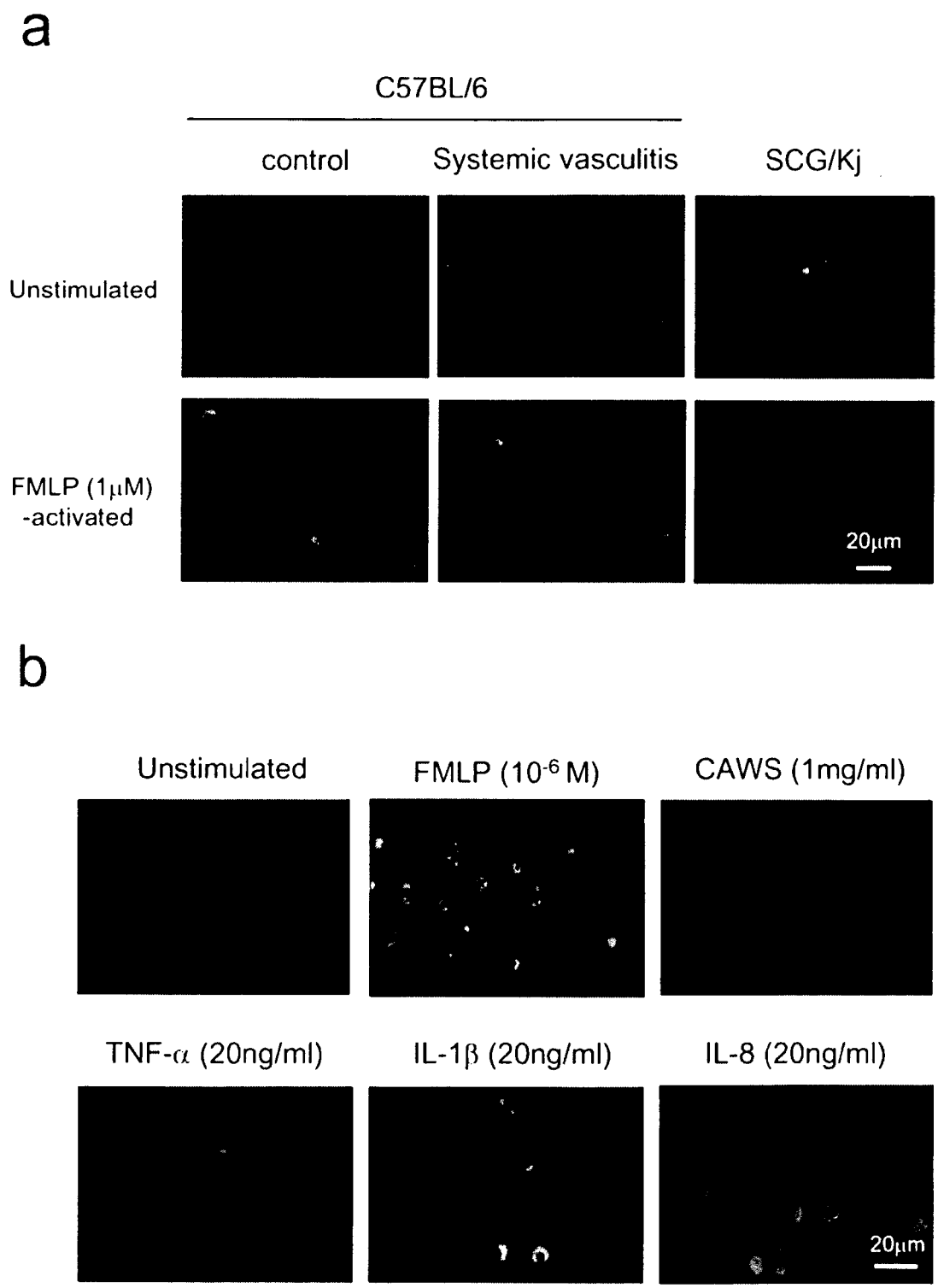

Fig. 5. MPO translocation on neutrophil membranes. The MPO translocation in murine and human neutrophils. *a*, Murine peritoneal neutrophils of naïve C57BL/6 mice, mice with ANCA-induced vasculitis, and aged (13 wks, male) SCG/Kj mice. Peripheral neutrophils were collected, stained with ANCA-QD with or without stimulation with FMLP. Bars indicate 20 μm. *b*, MPO surface translocation of human neutrophils after stimulation of proinflammatory cytokines. Human neutrophils (2×10^5 cells/ml) were stimulated with 1 μM FMLP, 1 mg/ml CAWS mannoprotein, 20 ng/ml TNF-α, 20 ng/ml IL-1β, and 20 ng/ml IL-8 at the indicated concentrations for 10 min, stained with ANCA-QD, and observed with fluorescent microscopy. Bar indicates 20 μm.

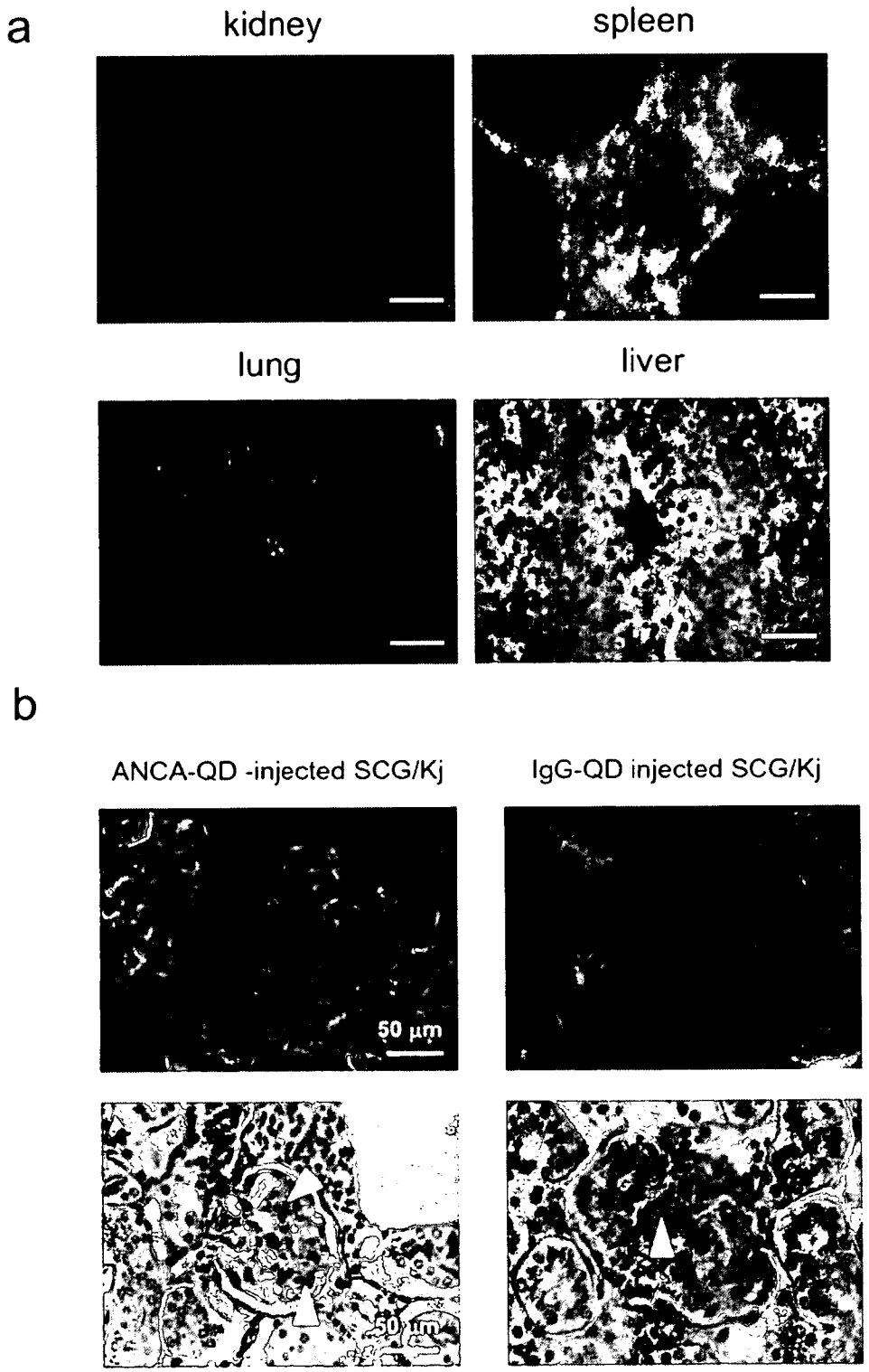

Fig. 6. Accumulation of ANCA-QD in the glomerulus with infiltrated neutrophils of SCG/Kj spontaneous glomerulonephritis mice. *a*, 1 mg of ANCA-QD were injected to the aged (13 wks old) SCG/Kj mice. The mice were sacrificed 24 hr after injection. Then collected spleen, lung, liver, and kidney were sliced to cryosection of 4 μm thickness. QD luminescence was observed with fluorescent microscopy. Bars indicate 250 μm. *b*, Fluorescent microscopic images (upper) and H&E stain (lower) of kidney cryosection of ANCA-QD-treated mice (left) and control IgG-QD-treated mice (right). Bars indicate 50 μm. The arrowheads indicate infiltrated segmented granulocytes.

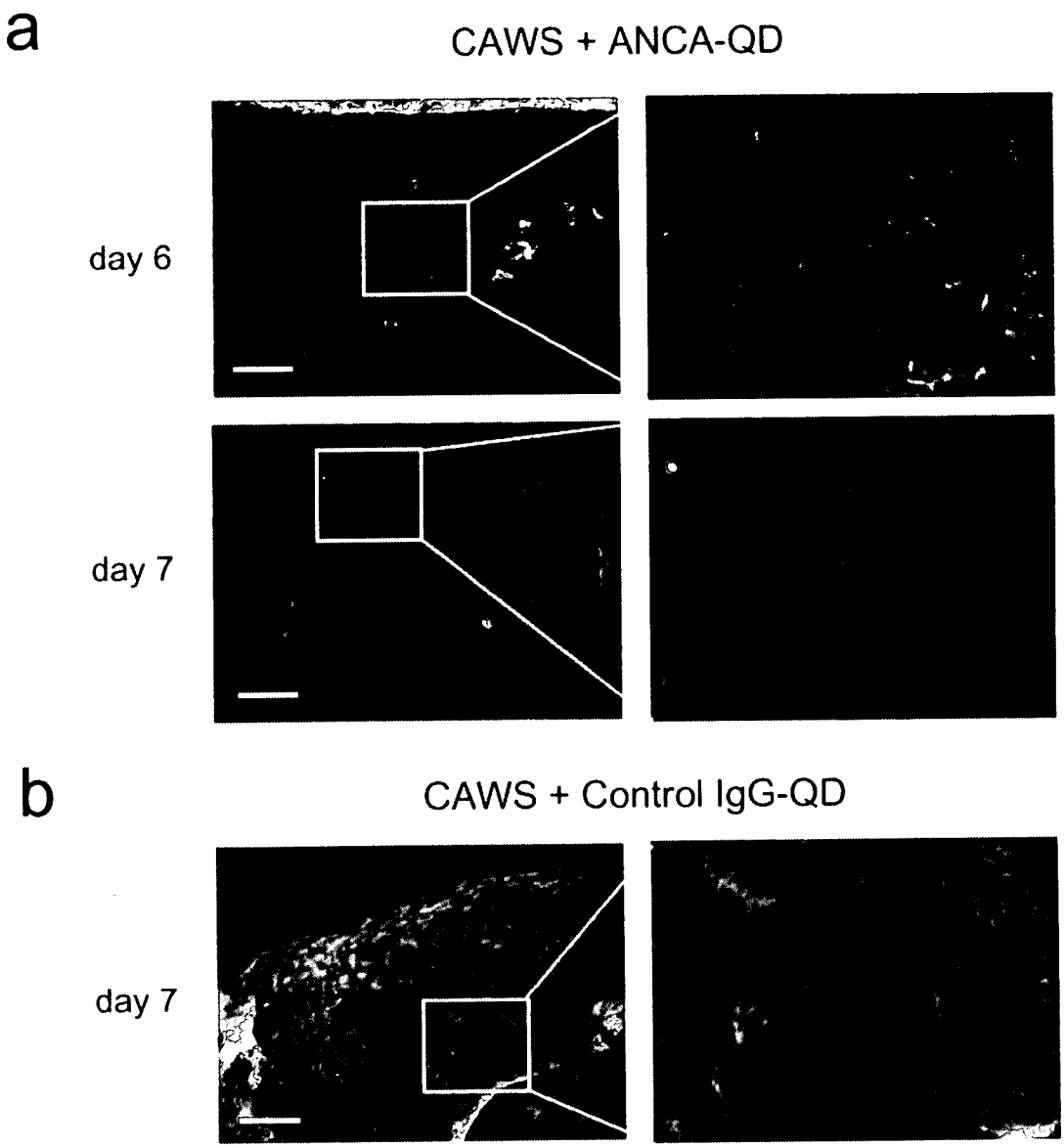

Fig. 7. Accumulation of ANCA-QD in the glomerulus with infiltrated neutrophils of MPO-ANCA-treated systemic vasculitis mice. Murine systemic vasculitis was induced in C57BL/6J mice as described in "Materials and Methods." In the case of second Ab injection, 250 μg of ANCA-QD were mixed with 1 mg of MPO-ANCA (*a*) or 250 μg of control IgG-QD were mixed with 1 mg of normal IgG, and injected to the primed mice. The mice were sacrificed 24 hr (day 6) and 48 hr (day 7) after second Ab-injection. Then collected kidney was sliced to cryosection of 4 μm thickness. Fluorescence emitted from ANCA-QD was observed with fluorescent microscopy. Fluorescent photos of right lane was enlarged images of gated area of left images. The bars indicate 250 μm.

secondary on day 5 (schematics is shown in Fig. 1a). After second stimulation with ANCA-QD, ANCA-QD was detected in developed glomerulonephritis lesion not on day 6 but on day 7 (Fig. 7a). In contrast, no signal was observed when control IgG-QD was injected (Fig. 7b). Treatment with only ANCA-QD without CAWS stimulation showed neither accumulation of ANCA-QD in kidney and lung nor mesangioproliferated glomeruli (data not shown).

To further investigate whether MPO-ANCA is reacted with activated neutrophils, immunohistochemical staining was performed. $CD11b^+$ $Gr1^+$ neutrophils were infiltrated in both lung (Fig. 8a) and glomeruli (Fig. 8b). However in kidney, ANCA-QD was not merged with infiltrated $Gr1^+$ cells but were located in the fringe of glomeruli. This result suggests that